Strong-Field Fourier Transform Vibrational Spectroscopy of D_2^+ Using Few-Cycle Near-Infrared Laser Pulses

Toshiaki Ando, Atsushi Iwasaki, and Kaoru Yamanouchi*
Department of Chemistry, School of Science, The University of Tokyo, 7-3-1 Hongo, Bunkyo-ku, Tokyo 113-0033, Japan

(Received 3 March 2018; published 28 June 2018)

The photoionization of D_2 and dissociation of the resultant D_2^+ are monitored by pump-probe measurements using intense near-infrared few-cycle laser pulses. The yields of D_2^+ and D^+ recorded up to the pump-probe delay time of 527 ps exhibit oscillatory structures reflecting the motion of the created vibrational wave packet of D_2^+, and the Fourier transform of the data in time domain reveals the vibrational level separations with uncertainties of 0.0002–0.0097 cm^{-1}, showing a potential application of the strong-field pump-probe measurements to high-resolution spectroscopy of molecular ions.

DOI: 10.1103/PhysRevLett.120.263002

Recent advances in ultrashort pulsed laser technologies have enabled us to generate few-cycle intense laser pulses and attosecond pulses with which a variety of dynamical processes of molecules have been investigated in real time [1–8]. The dynamical processes in the time domain can carry the information in the frequency domain especially when a created wave packet exhibits oscillatory motion as shown in diatomic molecules [1–3] and polyatomic molecules [4,5]. As long as we monitor the motion of a vibrational wave packet in a bound molecular system for a sufficiently long pump-probe delay period, the resolution of the frequencies obtained from the Fourier transform of the time domain signals can become very high; that is, high-precision measurements of the vibrational frequencies become possible. It is challenging to raise the precision to as high as what has been achieved by high-resolution spectroscopic measurements by time-resolved measurements using ultrashort intense laser pulses.

In the present study, we perform pump-probe measurements of the oscillation of D_2^+ by using near-infrared few-cycle intense laser pulses. By monitoring the oscillation of the yields of D_2^+ and the oscillation of the yield of D^+ originating from the photodissociation of D_2^+, $D_2^+ \rightarrow D^+ + D$, we scan the pump-probe time delay up to 527 ps. From the Fourier transform of the data in the time domain, we show that the vibrational level separations of D_2^+ are determined with uncertainties less than 0.01 cm^{-1}, which is the highest precision ever achieved by frequency domain spectroscopic techniques, showing a potential of the strong-field Fourier transform (FT) spectroscopy as a promising tool for obtaining spectroscopic data with a high resolution.

In the case of HD^+, thanks to the existence of the dipole moment, −0.87 D [9], vibrational transitions are allowed, and the vibrational transition frequencies were determined with a precision of $\delta\nu/\nu = 10^{-9}$ by frequency-comb spectroscopy of HD^+ in a cold ion trap [10–12]. On the other hand, in the cases of H_2^+ and D_2^+, because there is no dipole moment, no vibrational transitions have been observed, and the vibrational level energies have been determined by photoelectron spectroscopy [13–15] and zero-kinetic energy (ZEKE) photoelectron spectroscopy [16–19], whose frequency resolutions have been around 1 cm^{-1} in most cases. Recently, PFI-ZEKE photoelectron spectroscopy of high-lying vibrational states near the dissociation limit on H_2^+ and D_2^+ were performed with an uncertainty of 0.06 and 0.02 cm^{-1}, respectively [18,19], and the lifetimes of the quasibound state were determined on the basis of spectral line broadening.

In theory, the vibrational level energies of hydrogen molecular ions have been obtained with the highest accuracy among those of molecular ion species. The *ab initio* calculations of the nonadiabatic energy and relativistic and radiative corrections have been obtained [20–24]. Because the accurate rovibrational energy levels obtained theoretically are available, the validity of the frequencies and their uncertainties obtained experimentally in the present study can be examined by a comparison with the theoretical data.

Figure 1 shows the adiabatic potential energy curves of D_2^+. Through the ionization of D_2 by the pump pulse, the rovibrational wave packets of D_2^+ can be produced in the Franck Condon region of the electronic ground $^2\Sigma_g^+$ state, and then the wave packet starts oscillating under the absence of the laser pulse. Because the three-photon resonance and the one-photon resonance are located in a longer internuclear distance region than the equibrium internuclear distance, the wave packet at the outer turning point can be excited by the probe pulse with a higher probability than the wave packet at the inner turning point. In addition, because the transition between $^2\Sigma_g^+$ and $^2\Sigma_u^+$ is a parallel transition, D_2^+ molecules whose molecular axis is

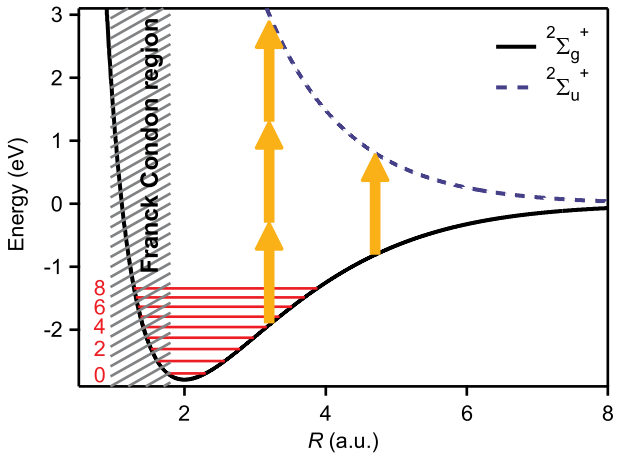

FIG. 1. Potential energy curves of the electronic ground $^2\Sigma_g^+(1s\sigma_g)$ state (black curve) and the first electronically excited $^2\Sigma_u^+(2p\sigma_u)$ state (blue broken curve) of D_2^+ measured from the dissociation limit. The vibrational energy levels are shown in the red horizontal lines.

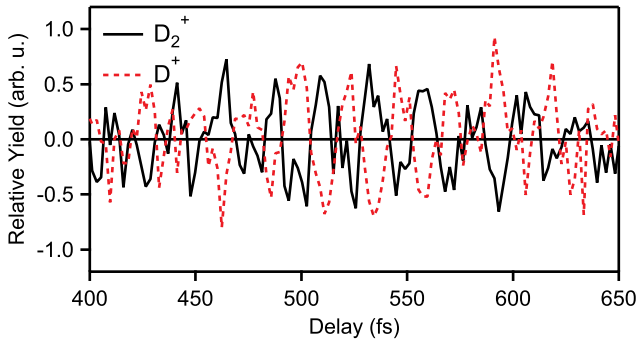

FIG. 2. Ion yields of D_2^+ (black solid line) and D^+ (red broken line) as a function of the time delay.

parallel to the laser polarization direction can be efficiently excited by the probe pulse. The wave packet prepared by the probe pulse on the dissociative potential curve, $^2\Sigma_u^+$, decomposes into D^+ and D. Because the excitation probability depends on the internclear distance and the angle between the molecular axis and the polarization direction of the probe pulse, it is expected that variations of the ion yields of D_2^+ and/or D^+ reflect the motion of the rotational and vibrational wave packet. Therefore, from the Fourier transform of the ion yields, the rotational and vibrational frequencies of D_2^+ can be obtained. The obtained frequencies are expected to be assigned to the rotational and vibrational frequencies under the absence of the laser pulse, because there are no laser fields during the delay time.

The detail of the experimental setup is described in Supplemental Material [25], Sec. I. Linearly polarized few-cycle intense laser pulses were generated by using a hollow-core fiber compression technique. The few-cycle intense laser pulses were introduced into a Michelson interferometer to produce pump and probe laser pulses. These pulses (5 fs, 780 nm, focal intensity 3.2×10^{14} W/cm^2) were focused onto an effusive molecular beam of D_2 in a time-of-flight mass spectrometer (TOF MS). The signal from the TOF MS was sent to two boxcar integrators to obtain the ion yields of D_2^+ and D^+. The delay time between the two pulses, Δt, was varied up to 527 ps by using an optical stage in the interferometer. In order to measure the delay time precisely, He-Ne laser light was sent to the interferometer in a parallel configuration with the few-cycle laser pulse. The interferometric signals of the He-Ne laser light detected by two photodiodes and the output signals from the boxcar integrators were recorded simultaneously. After the measurement, the number of fringes in the interferometric signals was counted and converted into the time delay.

Figure 2 shows the ion yields of D^+ and D_2^+ as a function of the time delay range from 400 to 650 fs. The ion yields of D^+ and D_2^+ oscillate with a period of ~25 fs, and the amplitudes of the yield oscillations of D^+ and D_2^+ are almost the same, but their phases are flipped by π from each other. The antiphase oscillation can be ascribed to the oscillation of the wave packet, which periodically produces D^+ through the decomposition process of D_2^+, $D_2^+ \rightarrow D^+ + D$, as explained above.

In order to obtain the FT spectra, the ion yields in the time delay range of 370 fs $< \Delta t <$ 527 ps were Fourier transformed. Because the few-cycle laser pulses have a pedestal structure in the range between -100 and $+100$ fs, the ion yield in the time delay range of 0 fs $< \Delta t <$ 370 fs was not used in the FT analysis in order that the interference between the pump and probe pulses does not give any influence on the FT spectra. Figure 3 shows the FT spectra of the ion yields. The peaks appearing in the FT spectra can be assigned to the rovibrational energy separations of D_2^+ and D_2, originating from the quantum beats among the rovibrational levels of D_2^+ and D_2. The peak frequencies correspond to the differences among the rovibrational energy separations of D_2^+, $E^+(v^{+\prime\prime}, N^{+\prime\prime}) - E^+(v^{+\prime}, N^{+\prime})$, and D_2, $E(v'', N'') - E(v', N')$. Indeed, in the FT spectra of the yield of D_2^+ and D^+, peaks assigned to the rotation level separations ($\Delta v^+ = 0$, $\Delta N^+ = 2, 4$) of D_2^+ are observed in the frequency range from 0 to 700 cm^{-1}, peaks assigned to the vibration level separations ($\Delta v^+ = 1$, $\Delta N^+ = 0, \pm 2, \pm 4$) of D_2^+ are observed in the frequency range from 800 to 1800 cm^{-1}, and peaks assigned to the vibrational separations corresponding to the vibrational overtones ($\Delta v^+ = 2$, $\Delta N^+ = 0, \pm 2$) of D_2^+ are observed in the frequency range from 2300 to 2960 cm^{-1}.

In addition, seven rotational level separations ($N' = 0$–6, $\Delta v = 0$, $\Delta N = 2$) of neutral D_2 are observed in the frequency range from 170 to 870 cm^{-1}, and seven vibrational level separations ($N' = 0$–6, $\Delta v = 1$, $\Delta N = 0$) of neutral D_2 are observed in the frequency range from

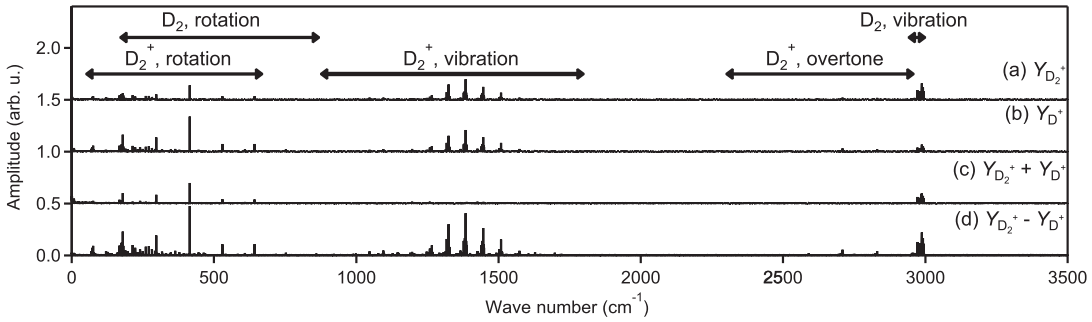

FIG. 3. Fourier transform spectra. The absolute value of the discrete Fourier transform of the yield of D_2^+ (a), the yield of D^+ (b), the sum of the yield of D_2^+ and D^+ (c), and the difference of the yield of D_2^+ and D^+ (d) are shown.

2940 to 3000 cm^{-1}. These peaks originating from the quantum beats of neutral D_2 indicate that the pump pulse also creates the rovibrational wave packet of D_2 and that the yields of D_2^+ and D^+ depend on the internuclear distance as well as on the angle between the molecular axis and the laser polarization direction.

If we perform the Fourier transform after taking the sum of the ion yields of D_2^+ and D^+, the peaks in the Fourier transform spectra assigned to D_2^+ have a significantly small amplitude. This is because the oscillation of the ion yield of D_2^+ and that of D^+ are antiphase. If we perform the Fourier transform after taking the difference of the ion yields of D_2^+ and D^+, the signal-to-noise (S/N) ratio of the peaks in the Fourier transform spectrum is higher than that achieved when only either one of the yield of D_2^+ or the yield of D^+ is Fourier transformed. Therefore, the Fourier transform of the yield difference between D_2^+ and D^+ is used for determining the vibrational energy separations in the analysis below.

The frequency axis of the FT spectra was calibrated by comparing the obtained peak positions assigned to the vibrations of D_2 ($N = 0$, 1, 2) with the previously experimentally obtained frequencies [26]. The vibration frequencies were obtained by fitting these peaks with a sinc function (see Supplemental Material [25], Sec. II). The uncertainties (1σ) of the frequencies of all the peaks assigned in this study are less than 0.01 cm^{-1}, and the smallest uncertainty is 2×10^{-4} cm^{-1}. The distribution of the deviations between the obtained frequencies obtained here and the calculated frequencies obtained in Ref. [20] exhibits a distribution close to a normal distribution, showing that no systematic errors are introduced in the energy calibration procedure in the present study.

As shown in Table I, the obtained vibration frequencies of D_2^+, $\Delta G(v^+ + 1/2) = E^+(v^+ + 1, 0) - E^+(v^+, 0)$, were compared with previous calculations [20], whose accuracy is considered to be 1×10^{-4} cm^{-1}. All the observed vibrational frequencies are summarized in Supplemental Material [25], Sec. III. The uncertainties of the frequencies are less than the magnitude of the relativistic corrections (~0.02 cm^{-1}) and that of the radiative corrections (~0.005 cm^{-1}) introduced in the theoretical calculations except for $\Delta G(1/2)$. Furthermore, the obtained frequencies are in good agreement with those obtained by the calculation [20]. Therefore, the uncertainties of the present experimental data are sufficiently small so that they are compared with the theoretically obtained relativistic and radiative corrections.

Figure 4 shows the expanded view of the FT spectrum in the frequency range from 1300 to 1400 cm^{-1}. The peak assigned to $N^+ = 2$, whose frequency is determined to be 1384.6896(2) cm^{-1}, has the largest peak amplitude among the peaks assigned to the vibrational energy separations of D_2^+ observed in this frequency range, which can be explained by the fact that $N = 2$ of neutral D_2 has the

TABLE I. Comparison of the vibrational separations of D_2^+, $\Delta G(v^+ + 1/2)(cm^{-1})$.

v^+	Exp.[a]	Calc.[b]	Exp.—Calc.
0	1577.0911(72)	1577.0904	0.0007
1	1512.4033(19)	1512.3993	0.0040
2	1449.3426(11)	1449.3429	−0.0003
3	1387.7523(6)	1387.7518	0.0005
4	1327.4621(9)	1327.4614	0.0007
5	1268.3099(22)	1268.3100	−0.0001

[a]This study (experimental).
[b]Reference [20].

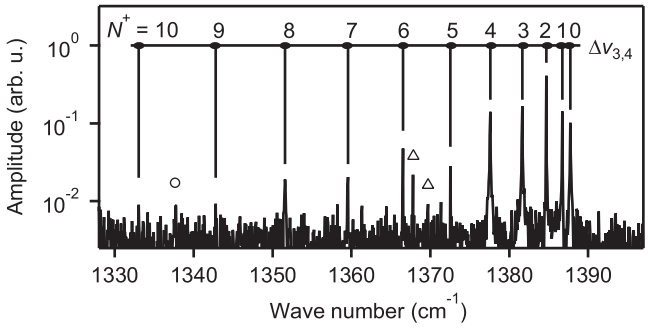

FIG. 4. Q branch of D_2^+ (1330–1390 cm^{-1}). ○, O branch ($\Delta v^+ = 1$, $\Delta N^+ = -2$); △, S branch ($\Delta v^+ = 1$, $\Delta N^+ = 2$).

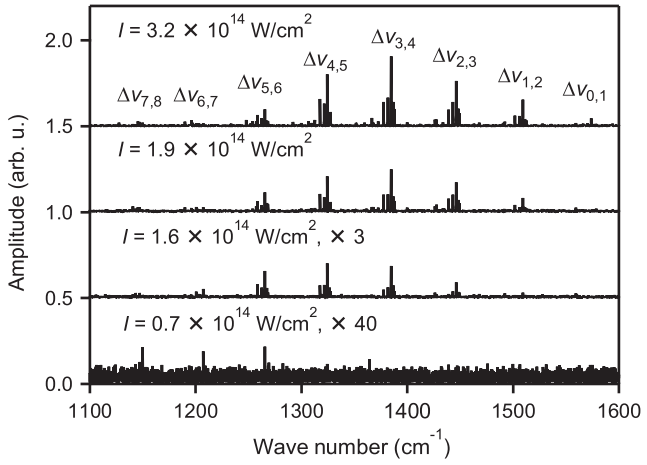

FIG. 5. Intensity dependence of the FT spectra.

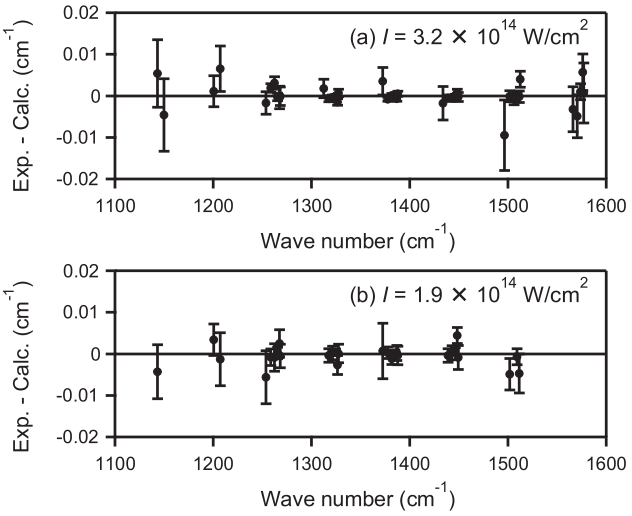

FIG. 6. The difference between the experiment and the calculation for $N^+ < 6$.

largest population among the rotational levels of D_2 at room temperature. However, the peak amplitudes of the vibrational energy separations for the higher rotational states are larger than that expected from the Boltzmann distribution. For instance, the amplitude of the peak for $N^+ = 6$ is around 12% of that for $N^+ = 2$, although the population of $N = 6$ should be around only 1.6% of that of $N = 2$ in the Boltzmann distribution. This larger population in the rotationally excited state than in the initial Boltzmann distribution at room temperature originates from the impulsive stimulated Raman excitation induced by the pump pulse. Therefore, vibrational energy separations for rotationally highly excited states can be determined by this type of strong-field high-resolution spectroscopy.

Figure 5 shows the dependence of the FT spectra on the laser field intensity. When the laser field intensity decreases, the intensities of the peaks assigned to the vibrational level separations for the lower vibrational levels decrease, and, at the focal intensity of 0.7×10^{14} W/cm^2, only the peaks for the higher vibrational states ($v^{+\prime} > 4$) are identified. This light-field intensity dependence can be explained by using light-dressed potential energy surfaces [28–31]. When the intensity of the probe pulse is weak, the dissociation into $D^+ + D$ proceeds only from the higher vibrational states of D_2^+ through the mechanisms called bond softening and below-threshold dissociation, and, therefore, only the peaks for the higher vibrational levels can appear in the FT spectrum. As the light-field intensity increases, the three-photon crossing point opens, and the dissociation starts proceeding through the lower-lying vibrational levels through the mechanism called above-threshold dissociation, and, consequently, the peaks for the lower vibrational levels also appear in the FT spectrum. The details of the light-field intensity dependence in the dissociation processes of light-dressed D_2^+ are described in Supplemental Material [25], Sec. IV.

So far, the frequencies for the vibrational energy separations have been regarded as the frequencies under field-free conditions. If the picosecond pulse contrast of the pump pulses and/or the probe pulses is poor, so that the tail part of the laser pulses persistently exist during the time duration between the pump and probe pulses, the frequencies of the peaks derived from the FT spectrum may be the frequencies of D_2^+ in the light field, which can be different from the frequencies of D_2^+ under field-free conditions because of the ac Stark effect [32,33]. However, even when the remaining light-field intensity in the tail part is as large as 1%, the frequency shifts of vibrational level energies originating from the ac Stark effect are expected to be at most 1.5×10^{-5} cm^{-1} for $\Delta G(1/2)$, which is sufficiently small compared with the uncertainties in the present measurements.

In order to examine the contribution from the tail part of the pump laser field to the vibration frequency, the peak frequencies derived from the FT spectra obtained with the two different laser intensities at $I = 1.9 \times 10^{14}$ W/cm^2 and $I = 3.2 \times 10^{14}$ W/cm^2 are compared with the theoretically calculated frequencies as shown in Fig. 6. In both cases, the experimental frequencies agree well with the calculated frequency, and no specific differences can be identified between the two cases. (See Supplemental Material [25], Sec. V.) Therefore, it can be concluded that the contribution from the residual laser field in the tail part of the pump laser pulse is negligibly small.

In summary, we determine the vibrational energy separations of D_2^+ with a high precision within the uncertainty of 0.01 cm^{-1} by strong-field pump-probe high-resolution FT spectroscopy. This pump-probe scheme can be decomposed into the following four steps: (i) the creation of the vibrational wave packet of molecular cations through the strong-field ionization of neutral molecules, (ii) the field-free propagation of the wave packet during the pump-probe time delay, (iii) the electronic excitation achieved by the

probe pulse, whose probability depends on the internuclear distance and the angle between the molecular axis and the laser polarization direction, and (iv) the fragmentation of molecular ions whose decomposition pathway depends on the electronic states prepared by the probe pulse. Because these four steps are common in most of the pump-probe excitations of molecules, this strong-field pump-probe high-resolution FT spectroscopy has a general applicability to the determination of vibrational energy separations of molecular ions with a high precision. Furthermore, the high-resolution data give us an opportunity to determine the lifetimes of quasibound rotational and vibrational levels created by the interaction with the strong pump laser pulse on the basis of spectral line broadening. If we could increase the spectral resolution more by extending the delay time range in the strong-field FT spectroscopy to the uncertainty of $\delta\nu/\nu = 10^{-10}$, we would be able to determine experimentally the electron-proton mass ratio, one of the fundamental physical constants [24].

The present research was supported by the following grant from the Ministry of Education, Culture, Sports, Science and Technology (MEXT), Japan: Grants-in-Aid for Specially Promoted Research (No. 15H05696).

*Corresponding author.
kaoru@chem.s.u-tokyo.ac.jp

[1] T. Ergler, A. Rudenko, B. Feuerstein, K. Zrost, C. D. Schröter, R. Moshammer, and J. Ullrich, Phys. Rev. Lett. **97**, 193001 (2006).
[2] S. De, M. Magrakvelidze, I. A. Bocharova, D. Ray, W. Cao, I. Znakovskaya, H. Li, Z. Wang, G. Laurent, U. Thumm, M. F. Kling, I. V. Litvinyuk, I. Ben-Itzhak, and C. L. Cocke, Phys. Rev. A **84**, 043410 (2011).
[3] T. Okino, Y. Furukawa, Y. Nabekawa, S. Miyabe, A. A. Eilanlou, E. J. Takahashi, K. Yamanouchi, and K. Midorikawa, Sci. Adv. **1**, e1500356 (2015).
[4] Z. Wei, J. Li, L. Wang, S. T. See, M. H. Jhon, Y. Zhang, F. Shi, M. Yang, and Z. H. Loh, Nat. Commun. **8**, 735 (2017).
[5] T. Ando, A. Shimamoto, S. Miura, A. Iwasaki, K. Nakai, and K. Yamanouchi, Commun. Chem. **1**, 7 (2018).
[6] A. Hishikawa, A. Matsuda, M. Fushitani, and E. J. Takahashi, Phys. Rev. Lett. **99**, 258302 (2007).
[7] A. Trabattoni, M. Klinker, J. González-Vázquez, C. Liu, G. Sansone, R. Linguerri, M. Hochlaf, J. Klei, M. J. J. Vrakking, F. Martín, M. Nisoli, and F. Calegari, Phys. Rev. X **5**, 041053 (2015).
[8] T. Ando, A. Shimamoto, S. Miura, K. Nakai, H. Xu, A. Iwasaki, and K. Yamanouchi, Chem. Phys. Lett. **624**, 78 (2015).
[9] P. R. Bunker, Chem. Phys. Lett. **27**, 322 (1974).
[10] J. C. J. Koelemeij, B. Roth, A. Wicht, I. Ernsting, and S. Schiller, Phys. Rev. Lett. **98**, 173002 (2007).
[11] U. Bressel, A. Borodin, J. Shen, M. Hansen, I. Ernsting, and S. Schiller, Phys. Rev. Lett. **108**, 183003 (2012).
[12] J. Biesheuvel, J. P. Karr, L. Hilico, K. S. E. Eikema, W. Ubachs, and J. C. J. Koelemeij, Nat. Commun. **7**, 10385 (2016).
[13] J. E. Pollard, D. J. Trevor, J. E. Reutt, Y. T. Lee, and D. A. Shirley, J. Chem. Phys. **77**, 34 (1982).
[14] W. Peatman, F. P. Wolf, and R. Unwin, Chem. Phys. Lett. **95**, 453 (1983).
[15] G. Öhrwall and P. Baltzer, Phys. Rev. A **58**, 1960 (1998).
[16] S. Stimson, Y. Chen, M. Evans, C. Liao, C. Y. Ng, C.-W. Hsu, and P. Heimann, Chem. Phys. Lett. **289**, 507 (1998).
[17] C. Chang, C.-Y. Ng, S. Stimson, M. Evans, and C. W. Hsu, Chin. J. Chem. Phys. **20**, 352 (2007).
[18] M. Beyer and F. Merkt, Phys. Rev. Lett. **116**, 093001 (2016).
[19] M. Beyer and F. Merkt, J. Phys. B **50**, 154005 (2017).
[20] R. E. Moss, J. Chem. Soc., Faraday Trans. **89**, 3851 (1993).
[21] J. P. Karr and L. Hilico, J. Phys. B **39**, 2095 (2006).
[22] Y. Ning and Z. C. Yan, Phys. Rev. A **90**, 032516 (2014).
[23] V. I. Korobov, Phys. Rev. A **77**, 022509 (2008).
[24] V. I. Korobov, L. Hilico, and J. P. Karr, Phys. Rev. Lett. **112**, 103003 (2014).
[25] See Supplemental Material at http://link.aps.org/supplemental/10.1103/PhysRevLett.120.263002 for experimental details on methods, analysis, and summary of obtained vibrational frequencies, which includes Refs. [20,26,27].
[26] M. L. Niu, E. J. Salumbides, G. D. Dickenson, K. S. E. Eikema, and W. Ubachs, J. Mol. Spectrosc. **300**, 44 (2014).
[27] L. Wolniewicz and T. Orlikowski, Mol. Phys. **74**, 103 (1991).
[28] A. Zavriyev, P. H. Bucksbaum, H. G. Muller, and D. W. Schumacher, Phys. Rev. A **42**, 5500 (1990).
[29] A. Giusti-Suzor, F. H. Mies, L. F. DiMauro, E. Charron, and B. Yang, J. Phys. B **28**, 309 (1995).
[30] I. Maruyama, T. Sako, and K. Yamanouchi, J. Phys. B **37**, 3919 (2004).
[31] S. Jiang, C. Yu, G. Yuan, T. Wu, and R. Lu, Sci. Rep. **7**, 42086 (2017).
[32] W. Kołos and L. Wolniewicz, J. Chem. Phys. **46**, 1426 (1967).
[33] S. Schiller, D. Bakalov, A. K. Bekbaev, and V. I. Korobov, Phys. Rev. A **89**, 052521 (2014).